Polymer Degradation and Stability 107 (2014) 98–105

Contents lists available at ScienceDirect

Polymer Degradation and Stability

journal homepage: www.elsevier.com/locate/polydegstab

Pyrolysis route of a novel flame retardant constructed by phosphaphenanthrene and triazine-trione groups and its flame-retardant effect on epoxy resin

Lijun Qian*, Yong Qiu, Nan Sun, Menglan Xu, Guozhi Xu, Fei Xin, Yajun Chen

Department of Materials Science & Engineering, Beijing Technology and Business University, Beijing 100048, PR China

ARTICLE INFO

Article history:
Received 3 September 2013
Received in revised form
23 April 2014
Accepted 8 May 2014
Available online 24 May 2014

Keywords:
Flame retardant
DOPO
Triazine-trione
Synergistic effect
Epoxy resin

ABSTRACT

A novel flame retardant TGIC-DOPO, which was constructed by phosphaphenanthrene and triazine-trione groups, was synthesized via a controllable ring-opening addition reaction between 1,3,5-triglycidyl isocyanurate (TGIC) and 9,10-dihydro-9-oxa-10-phosphaphenanthrene-10-oxide (DOPO). The flame-retardant effect of TGIC-DOPO on an epoxy resin, diglycidyl ether of bisphenol-A (DGEBA), cured with 4,4′-diamino-diphenyl sulfone was investigated. The results of the limited oxygen index (LOI), UL94 vertical burning test, and cone calorimeter test indicated that the TGIC-DOPO imparted flame-retardant properties to DGEBA thermosets. When the mass fraction of TGIC-DOPO reached 12wt.%, the DGEBA thermoset acquired a LOI value of 33.3%, UL94 V-0 rating, and the lower peak of heat release rate (pk-HRR) at 481 kW/m^2. Specifically, the DGEBA thermoset with 6wt.% TGIC-DOPO had an LOI value of 33.3%, whereas the DGEBA thermoset with 10wt.% TGIC-DOPO had the highest LOI value of 35.2% among the specimens. Meanwhile, the time to ignition, pk-HRR, average of effective heat of combustion (av-EHC), and total heat release of the DGEBA thermoset were all negatively correlated with the mass fraction of TGIC-DOPO. Moreover, the average CO_2 and CO yields exhibited a downtrend with increasing mass fraction of TGIC-DOPO from 6wt.%. The reduction of av-EHC with increase of TGIC-DOPO content in thermosets confirmed the free radical quenching effect of TGIC-DOPO in gaseous phase during combustion. The macromorphology, micromorphology and element content of the residues from the cone calorimeter test revealed the bi-phase flame-retardant effect of TGIC-DOPO. Furthermore, the pyrolysis route of TGIC-DOPO were investigated via Py-GC/MS, which disclosed that the decomposed TGIC-DOPO with double flame-retardant groups released various fragments with quenching effect on free radical chain reaction of combustion. The fragments enhanced the flame-retardant performance of DGEBA thermosets both in gaseous and condensed phases. The flame-retardant performance of TGIC-DOPO was resulted by the quenching effect of TGIC-DOPO and the synergistic effect of phosphaphenanthrene and triazine-trione groups.

© 2014 Elsevier Ltd. All rights reserved.

1. Introduction

In the past several decades, epoxy resin has been rapidly and significantly developed in theory and in practical application [1–5]. In the electronic and electrical industry, various epoxy resins are used as adhesives [6,7] and electrical encapsulation materials [8,9] because of their excellent electrical insulation and adhesive properties as well as corrosion resistance. However, most epoxy resins are flammable, which pose potential risks. Thus, to impart flame-retardant properties to epoxy resin is necessary for its practical demands [10,11].

The synthesis of novel phosphorus-containing flame-retardant additives and the preparation of phosphorus-containing flame-retardant epoxy resins have already been conducted [12–15]. To obtain a highly efficient flame-retardant epoxy resin, several flame-retardant chemical structures composed of single or multiple flame-retardant functional groups have been utilized, such as phosphaphenanthrene [16–18], cyclotriphosphazene [19,20], phosphorus-containing silsesquioxane [21], pentaerythritol diphosphonate [22,23], triazine [24,25], and triazine-trione [26–28] structures. Moreover, several novel flame retardant

* Corresponding author. Zonghe Building No. 403, Fucheng Road No. 33, Haidian District, Beijing, China. Tel./fax: +86 10 68984719.
E-mail addresses: qianlj@th.btbu.edu.cn, augusqian@163.com (L. Qian).

http://dx.doi.org/10.1016/j.polymdegradstab.2014.05.007
0141-3910/© 2014 Elsevier Ltd. All rights reserved.

additive structures with a high flame-retardant efficiency have been discovered for the synergistic effect of flame retardant groups [20,29].

In the present work, a novel addition-type flame retardant TGIC-DOPO, which was based on phosphaphenanthrene and triazine-trione groups, was prepared via a one-step controllable ring-opening addition reaction. Then, the epoxy resin thermosets incorporated TGIC-DOPO were investigated to evaluate the flame-retardant behavior. The pyrolysis route of TGIC-DOPO was also explored to find out its flame-retardant mechanism on epoxy resin thermosets.

2. Experimental

2.1. Materials

1,3,5-Triglycidyl isocyanurate (TGIC) was provided by Shanghai Fangruida Chemical Co. Ltd., China. 9,10-Dihydro-9-oxa-10-phosphaphenanthrene-10-oxide (DOPO) was supplied by Shanghai Eutec Chemical Co., China. The epoxy resin, diglycidyl ether of bisphenol-A (DGEBA, commercial name: E-51), was purchased from Blue Star New Chemical Material Co. Ltd., China. 4,4′-Diamino-diphenyl sulfone (DDS) was purchased from Sinopharm Chemical Reagent Co. Ltd., China.

2.2. Synthesis of TGIC-DOPO

DOPO (63.7 g, 0.295 mol) was melted at 135 °C with mechanical stirring in a three-neck flask. After the DOPO was completely melted, TGIC (29.7 g, 0.100 mol) was added into the reaction system at the rate of 2.97 g per 20 min. The reaction temperature was then elevated to 170 °C within 30 min, and the mixture was stirred for 3 h. The white powders of TGIC-DOPO were obtained after the cooled products were grinded at room temperature. The products were refined by washing with toluene and then drying. The reaction formula is shown in Scheme 1. The yield was >98.2%. The purity of TGIC-DOPO was 93.6% investigated by high performance liquid chromatography (HPLC). The impurities were mainly from incomplete addition reaction between TGIC and DOPO. The obtained peaks in the Fourier transform infrared (FT-IR) spectra (KBr, cm^{-1}) were 3369 (OH), 3065 (Ar—H), 2905 (C—H), 1690 (C═O), 1595 (C_6H_6), 1464 (C—N), 1203 (P═O), 915 (P-O-Ph), and 756 (o-R_1-Ph-R_2). The ^{1}H nuclear magnetic resonance (^{1}H NMR) data obtained (DMSO-d_6, ppm) were δ = 7.1 to 8.3 (Ar—H, 24H), δ = 5.1 and 5.4 (CH, 3H), δ = 3.8 and 4.2 (DOPO-CH_2, 6H), δ = 3.7 ($C_3N_3O_3$—CH_2, 6H), and δ = 2.1 to 2.3 (OH, 3H). The ^{31}P nuclear magnetic resonance (^{31}P NMR) datum obtained (DMSO-d_6, ppm) was δ = 35.9.

2.3. Preparation of flame retardant DGEBA and the control sample

DGEBA and TGIC-DOPO were heated to 185 °C and stirred until TGIC-DOPO was completely dissolved in DGEBA. DDS was then added into the mixture at 185 °C and blended thoroughly. After the mixture was degassed at 185 °C for 3 min, it was poured into preheated molds and cured at 150 °C for 3 h and then at 180 °C for 5 h. The samples were labeled as 6%TGIC-DOPO/DGEBA/DDS, 8% TGIC-DOPO/DGEBA/DDS, 10%TGIC-DOPO/DGEBA/DDS, and 12% TGIC-DOPO/DGEBA/DDS based on the mass fraction of TGIC-DOPO in the DGEBA thermoset. The control sample, DGEBA/DDS, was also prepared in the same manner but without the addition of the flame retardant TGIC-DOPO. The formulations of DGEBA, DDS, and TGIC-DOPO in each epoxy resin thermosets are listed in Table 1.

2.4. Characterizations

FT-IR spectra were obtained using a Nicolet iN10MX-type spectrometer. The powdered samples were thoroughly mixed with KBr and then pressed into pellets. The ^{1}H NMR and ^{31}P NMR data were obtained using a Bruker AV300MB NMR spectrometer and a DMSO-d_6 solvent.

The purity of TGIC-DOPO was investigated by Shimadzu HPLC LC10AT with C-18 column. The detection wavelength was 254 nm. The mobile phase was the mixture of methanol and water, whose volume ratio was 90:10. The flowing rate of mobile phase was 1 mL/min.

The glass transition temperature (T_g) was determined under N_2 atmosphere by using a TA instrument Q100 differential scanning calorimeter. The thermal history of the TGIC-DOPO sample was eliminated by heating at 140 °C for 1 min and then cooling down to 40 °C at the rate of 10 °C/min. The T_g of sample was then determined by heating to 200 °C at 10 °C/min. The thermal history of the DGEBA thermoset samples were eliminated by heating at 210 °C for 1 min and then cooling down to 40 °C at 10 °C/min. The T_g of samples were then determined by heating to 250 °C at 10 °C/min. All the tests were repeated three times, and all of the T_g values were reproducible within ±3%.

Thermogravimetric analysis (TGA) was performed using a TA instrument Q5000 IR thermal gravimetric analyzer. The sample was placed in a platinum crucible and heated from 50 °C to 700 °C at the rate of 20 °C/min in N_2 atmosphere. All the tests were repeated three times, and the typical TGA data were reproducible within ±5%.

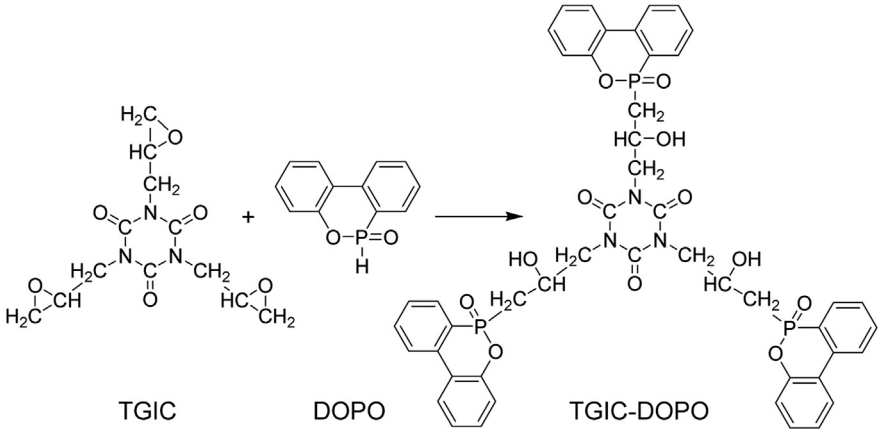

Scheme 1. Synthesis of TGIC-DOPO.

Table 1
Formulas of the DGEBA thermosets.

Samples	DGEBA (g)	DDS (g)	TGIC-DOPO	
			(g)	(wt.%)
DGEBA/DDS	100	31.6	–	–
6%TGIC-DOPO/DGEBA/DDS	100	31.6	8.6	6.1
8%TGIC-DOPO/DGEBA/DDS	100	31.6	11.6	8.1
10%TGIC-DOPO/DGEBA/DDS	100	31.6	14.9	10.2
12%TGIC-DOPO/DGEBA/DDS	100	31.6	18.3	12.2

The limited oxygen index (LOI) value was measured using an FTT (Fire Testing Technology, UK) Dynisco LOI instrument according to ASTM D2863-97 (sample dimension: 130 mm × 6.5 mm × 3.2 mm). The LOI measurement for each specimen was repeated three times, and their error values were ±0.3%. The vertical burning test for the UL94 combustion level was performed using an FTT0082 instrument according to ASTM D 3801 (sample dimension: 125 mm × 12.7 mm × 3.2 mm). The cone calorimeter test was performed using an FTT0007 cone calorimeter according to ISO5660 at an external heat flux of 50 kW/m^2 (sample dimension: 100 mm × 100 mm × 3 mm). The measurement for each specimen was repeated three times, and the error values of the typical cone calorimeter data were reproducible within ±5%.

The micromorphology images of the residues after cone calorimeter test were obtained using a FEI Quanta 250 FEG field-emission scanning electron microscope at high vacuum conditions with a voltage of 20 kV.

The element contents of residues from cone calorimeter test were investigated via a PerkineElmer PHI 5300 ESCA X-ray photoelectron spectrometer. The tested specimens were obtained from the sufficiently mixed and grinded residues, and the results were the average of the three times repeated tests which were all reproducible within ±5%.

To recognize the pyrolysis fragments of TGIC-DOPO, a Shimadzu GC-MS-QP5050A gas chromatography-mass spectrometer equipped with a PYR-4A pyrolyzer was employed. The helium (He) was utilized as carrier gas for the volatile products. The injector temperature was 250 °C, the temperature of GC/MS interface was 280 °C and the cracker temperature was 500 °C.

3. Results and discussion

3.1. Thermal analysis

The thermal properties of the samples are listed in Table 2. TGIC-DOPO has a T_g of 107 °C and hasn't melting point, which is caused by the bulky volume and non-planarity of phosphaphenanthrene group. It shows the amorphous characteristic of TGIC-DOPO. Compared with the neat DGEBA/DDS sample (T_g = 191 °C), the T_g values of the flame-retardant DGEBA thermosets gradually decreased with increasing mass fraction of TGIC-DOPO. This result is due to the fact that the T_g of TGIC-DOPO is at 107 °C, which induces the emergence of the T_g values of the thermosets at lower temperatures. Nevertheless, TGIC-DOPO only had a slight effect on the T_g value of DGEBA thermosets because the T_g value of 12%TGIC-DOPO/DGEBA/DDS was only reduced by 15 °C even if it had the largest amount of TGIC-DOPO in all the tested samples.

Table 2
The thermal parameters of TGIC-DOPO and DGEBA thermosets.

Samples	T_g (°C)	$T_{d,1\%}$ (°C)	$T_{d,\ 2\%}$ (°C)	Char yields at 700 °C (wt.%)
DGEBA/DDS	191	378	391	12.6
6%TGIC-DOPO/DGEBA/DDS	190	339	358	18.5
8%TGIC-DOPO/DGEBA/DDS	182	346	357	18.4
10%TGIC-DOPO/DGEBA/DDS	180	314	353	18.5
12%TGIC-DOPO/DGEBA/DDS	176	337	347	18.8
TGIC-DOPO	107	211	251	7.4

The TGA curves of all the thermosets are shown in Fig. 1, and some typical data are listed in Table 2. The onset degradation temperature ($T_{d,1\%}$) of the neat DGEBA/DDS sample was about 378 °C, whereas that of the TGIC-DOPO sample was about 211 °C. Hence, TGIC-DOPO was obviously decomposed before the DGEBA thermosets. TGIC-DOPO will affect the decomposition process of DGEBA thermosets. The evidence is as follows. The weight loss at 400 °C of DGEBA/DDS was about 4.3wt.%, whereas the weight losses of TGIC-DOPO/DGEBA/DDS at the same temperature were from 31.7wt.% to 48.6wt.% with increasing mass fraction of TGIC-DOPO (Fig. 1). At 400 °C, the weight losses of all the TGIC-DOPO/DGEBA/DDS specimens were much larger than the mass fraction of TGIC-DOPO in each TGIC-DOPO/DGEBA/DDS composite. It can be deduced that the pyrolysis of TGIC-DOPO in advance induced the decomposition of the DGEBA thermoset matrix. The induced decomposition effect can also be enhanced with increasing mass fraction of TGIC-DOPO. This behavior might be caused by the production of more free radicals from the decomposition of TGIC-DOPO. The free radicals result in earlier and faster decomposition of the matrix and greater weight loss of the matrix at lower temperature. Moreover, the char yields at 700 °C of all the samples show that the incorporation of TGIC-DOPO can obviously increase the charring yield of the matrix. When the mass fraction of TGIC-DOPO reached 6.0wt.%, the charring yield of 6%TGIC-DOPO/DGEBA/DDS at 700 °C increased to 18.5wt.%, but that of the DGEBA/DDS and TGIC-DOPO samples were 12.6wt.% and 7.4wt.% respectively. However, when the mass fraction of TGIC-DOPO was further increased, the char yield didn't rise obviously. This increase of char yield can be ascribed to the interaction between TGIC-DOPO and thermoset matrix. The charring behavior of the flame-retardant thermosets can be based on the ratio of phosphaphenanthrene, triazine-trione and matrix. When the matrix was constant, the unilateral increase in the phosphaphenanthrene and triazine-trione provided by TGIC-DOPO contributed less to the char yield of the thermosets.

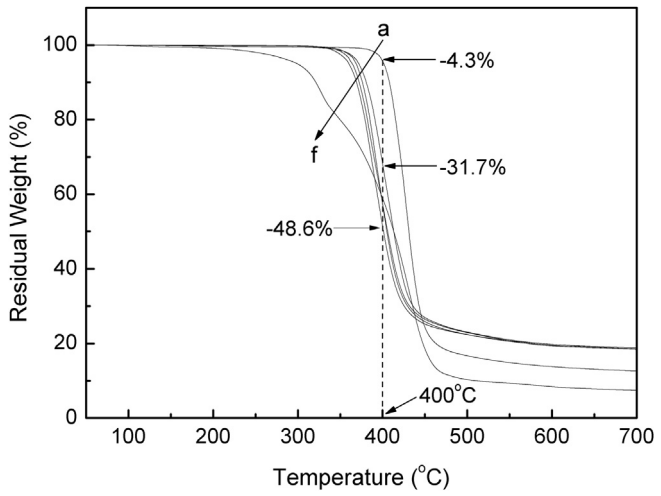

Fig. 1. TGA curves of DGEBA thermosets and TGIC-DOPO. (a) DGEBA/DDS; (b) 6%TGIC-DOPO/DGEBA/DDS; (c) 8%TGIC-DOPO/DGEBA/DDS; (d) 10%TGIC-DOPO/DGEBA/DDS; (e) 12%TGIC-DOPO/DGEBA/DDS; (f) TGIC-DOPO.

3.2. LOI and UL94 rating tests

The flame-retardant properties of the DGEBA thermosets were determined using LOI and UL94 vertical burning tests. The corresponding results are presented in Table 3. The LOI value of the neat DGEBA/DDS sample was only 22.5%, whereas the LOI value of 6% TGIC-DOPO/DGEBA/DDS sample increased to 33.3%. The LOI value of the specimens can be further increased by increasing the mass ratio of TGIC-DOPO in the thermosets. When the mass fraction of TGIC-DOPO was 10wt.%, the LOI value of 10%TGIC-DOPO/DGEBA/DDS increased to 35.2%. However, at higher amounts of TGIC-DOPO, the LOI value of the DGEBA thermosets slightly decreased. The remarkable character is the higher LOI value of thermoset with the lower TGIC-DOPO loadings. The LOI performance of TGIC-DOPO was better than that of DOPO and its derivatives [16,29] at the less loadings in the same DGEBA thermosets. It can be inferred that the excellent performance resulted by the special chemical structure, which is composed of phosphaphenanthrene [16–18] and triazine-trione [26–28] groups with certain flame-retardant effect. The flame-retardant groups and the matrix can interact to bring a better effect to the TGIC-DOPO/DGEBA/DDS system during combustion. Furthermore, the ratio between TGIC-DOPO containing phosphaphenanthrene and triazine-trione groups and the cured DGEBA matrix influenced more on the flame-retardant properties of thermosets. At a low mass fraction, an increase of TGIC-DOPO content in the DGEBA thermoset system contributed to the ratio optimization of flame-retardant contents, which caused the rise of LOI value. However, further increasing the TGIC-DOPO content resulted in a deviation from the optimal ratio of the flame-retardant contents, thereby resulting in a negative effect on the LOI performance of the thermosets.

The UL94 vertical burning test results indicate that the neat DGEBA/DDS sample cannot be rated according to the UL94 rule. The UL94 ratings of the DGEBA thermoset were enhanced with increasing mass fraction of TGIC-DOPO. When the mass fraction of TGIC-DOPO reached 6%, it hadn't any dripping observed during the vertical burning test although its UL94 rating was unrated. The phenomenon disclosed the excellent anti-dripping properties of TGIC-DOPO, which implied the formation of thick melt via a condensed-phase interaction between TGIC-DOPO and matrix during combustion. When the mass fraction of TGIC-DOPO was increased to 12wt.%, the 12%TGIC-DOPO/DGEBA/DDS sample reached the UL94 V-0 rating with the shorter burning time and without dripping. But the 10%TGIC-DOPO/DGEBA/DDS sample with the highest LOI value didn't reach the UL94 V-0 rating. The decrease of LOI value and increase of UL94 rating reveal that the flame-retardant action of TGIC-DOPO could obtain redistribution in gaseous phase and condensed phase when the mass fraction of TGIC-DOPO increased in DGEBA thermosets. The reason will be further discussed in the subsequent section.

3.3. Cone calorimeter test

Cone calorimetry test was conducted to investigate sufficiently the flame-retardant behaviors of TGIC-DOPO on the DGEBA thermosets. The curves of heat release rate (HRR) are shown in Fig. 2, and partial characteristic parameters, such as the time to ignition (TTI), average of heat release rate (av-HRR), peak of heat release rate (pk-HRR), average of effective heat of combustion (av-EHC), total heat release (THR), average CO yield (av-COY), and average CO_2 yield (av-CO_2Y), are summarized in Table 4.

As shown in Fig. 2 and Table 4, the TTIs of the thermosets were obviously shortened with the incorporation of TGIC-DOPO. The pk-HRRs also remarkably decreased with increasing mass fraction of TGIC-DOPO in the matrix. According to the previous discussion on TGA data and the subsequent Py-GC-MS results, the TGIC-DOPO molecules were easily decomposed to produce some free radicals at the lower temperature during the initial degradation. The free radicals then induced the matrix to degrade and release combustible volatiles, which weaken the ignition-resistance of the matrix. Thus, the TTIs of the samples were shortened. With the development of the thermal degradation process, the interaction of the products from the pyrolysis of TGIC-DOPO and the DGEBA thermoset jointly promoted charring of the matrix, and the interactions also enhanced the residue quantity and the melt toughness. The char layer inhibited the thermosets from burning and effectively hindered the heat from reaching the inner resin, which further restrained the pyrolysis of the matrix and decreased the combustion intensity to a low level.

Similarly, both av-EHC and THR decreased with increasing mass fraction of TGIC-DOPO (Table 4). EHC, which is the ratio of HRR to mass loss rate measured at a certain point, discloses the burning degree of volatile gases in gas-phase flame during combustion. In Table 4, the av-EHC value gradually decreased with the increase of TGIC-DOPO contents. This phenomenon further supported the flame-retardant effect of TGIC-DOPO in the gaseous phase because the more combustible volatiles and the less combustion heat generated during combustion can only be ascribed to the flame-retardant quenching effect from the gaseous-phase pyrolysis products of TGIC-DOPO. Av-EHC corresponds to the value of combustion heat from the ignition of gaseous-phase combustible volatiles, whereas THR corresponds to the total combustion heat from the ignition of gaseous- and condensed-phase combustibles. The decrease in THR values from 26.5% to 40.2% is much larger than that of av-EHC values, which just decreased from 8.3% to 29.2%. These results reveal that the combustion heat from the ignition of combustibles in the condensed phase was reduced more compared with that in the gaseous phase. Therefore, the incorporation of TGIC-DOPO in the matrix not only brings the better gaseous-phase flame-retardant effect but also results in more remarkable

Table 3
LOI value and UL94 rating of DGEBA thermosets.

Samples	LOI (%)	UL94	
		Rating	Dripping
DGEBA/DDS	22.5	Unrated	Yes
6%TGIC-DOPO/DGEBA/DDS	33.3	Unrated	No
8%TGIC-DOPO/DGEBA/DDS	34.3	V-1	No
10%TGIC-DOPO/DGEBA/DDS	35.2	V-1	No
12%TGIC-DOPO/DGEBA/DDS	33.3	V-0	No

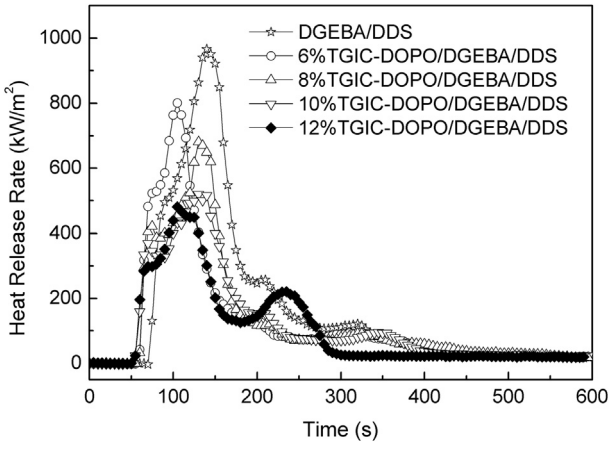

Fig. 2. Heat release rate curves of DGEBA thermosets.

Table 4
Cone calorimeter data of DGEBA thermosets.

Samples	TTI (s)	av-HRR (kW/m^2)	pk-HRR (kW/m^2)	av-EHC (MJ/kg)	THR (MJ/m^2)	av-COY (kg/kg)	av-CO_2Y (kg/kg)
DGEBA/DDS	65	194	966	24	102	0.095	2.087
6%TGIC-DOPO/DGEBA/DDS	54	135	800	22	75	0.154	1.940
8%TGIC-DOPO/DGEBA/DDS	54	141	680	20	76	0.151	1.753
10%TGIC-DOPO/DGEBA/DDS	50	131	520	19	71	0.140	1.521
12%TGIC-DOPO/DGEBA/DDS	48	113	481	17	61	0.135	1.482

condensed-phase flame-retardant effect. This mechanism will be further discussed in the subsequent section.

Table 4 also shows that the av-CO_2Y of 6%TGIC-DOPO/DGEBA/DDS decreased, whereas its av-COY increased with increasing mass fraction of TGIC-DOPO compared with that of DGEBA/DDS. The phenomenon is another evidence of the flame-retardant effect of TGIC-DOPO during combustion. When TGIC-DOPO was added at a low mass fraction, the induced degradation of matrix by TGIC-DOPO became obvious, thereby releasing more combustible volatiles into the gaseous phase at the start of the combustion. Meanwhile, the pyrolysis fragments with quenching effect from TGIC-DOPO restrained the ignition of combustible volatiles, thus resulting in more incomplete combustion products (CO) and less complete combustion products (CO_2). The reason of this behavior corresponds to that of the decrease in av-EHC. In addition, av-COY and av-CO_2Y decreased more when the mass fraction of TGIC-DOPO was further increased. It shows that the more TGIC-DOPO resulted in less released combustible volatiles and lower combustion intensity.

3.4. Morphology and element composition of the residues from cone calorimeter test

Fig. 3 shows the macromorphology images of the residues of the DGEBA thermosets from cone calorimeter test. The residue from the neat DGEBA/DDS sample was in a badly broken state. However, the residual char yields and expansion ratios of the other samples were markedly elevated with the incorporation of TGIC-DOPO. The interaction between the TGIC-DOPO and the DGEBA thermoset can be inferred to not only improve the melt toughness to seal more combustible volatiles and make residue expand but also increase the quantities of the residue (increase by 89%–115%).

To explore the flame-retardant charring mechanism further, SEM analysis was conducted. Fig. 4 typically shows the SEM images of the residue of neat DGEBA/DDS and 12%TGIC-DOPO/DGEBA/DDS samples from cone calorimeter test. Numerous open holes with different sizes in the residue of DGEBA/DDS are found in Fig. 4(a). The residue of 12%TGIC-DOPO/DGEBA/DDS [Fig. 4(b)] presents a sealed structure with an obvious stretched track, which indicates the excellent toughness of the melt. The open holes in the residue of DGEBA/DDS provided channels for the combustible volatiles generated from the inner matrix to the gaseous phase, thereby increasing the combustion intensity and the pyrolysis speed of the matrix. Thus, full combustion occurred. However, the sealed residue of 12%TGIC-DOPO/DGEBA/DDS can seal the combustible or incombustible volatiles in the residue, and then cut off the supply of fuel to weaken the combustion intensity.

Additionally, the element contents of the residues from the cone calorimeter tests were determined via XPS. The results are shown in Table 5. The phosphorus contents of all the residues increased with increasing mass fraction of TGIC-DOPO till 1.86wt.% in the residue of 12%TGIC-DOPO/DGEBA/DDS, which is most in all the samples. It confirms that the more phosphaphenanthrene groups containing phosphorus element from TGIC-DOPO interacted with the matrix and formed residue. Most of the phosphaphenanthrene groups of TGIC-DOPO exert a strong interaction with the DGEBA thermoset during combustion and promote the formation of phosphorus-rich residue, which enhances the toughness of the melt and then enlarges the condensed-phase flame-retardant effect on the DGEBA thermoset. On the contrary, the nitrogen contents of the residues reduced gradually with increasing mass fraction of TGIC-DOPO till 4.04wt.% in the residue of 12%TGIC-DOPO/DGEBA/DDS, which is least in all the samples. It confirms that the more triazine-trione groups containing nitrogen element were released into the gaseous phase and exerted the gaseous-phase flame retardant effect. The redistributed effect of the two flame-retardant groups in gaseous phase and condensed

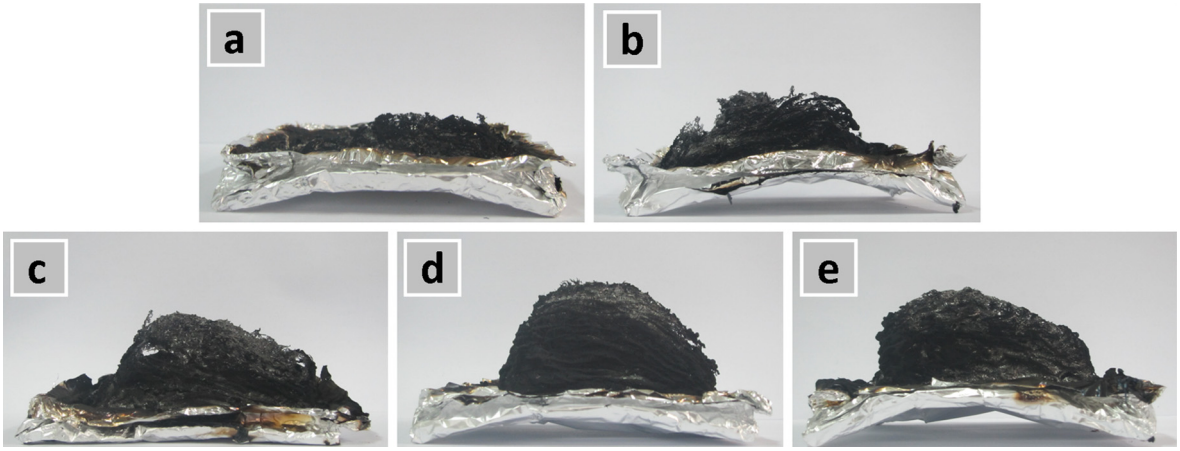

Fig. 3. Photos of cone calorimeter residues of DGEBA thermosets. (a) DGEBA/DDS, residual weight: 8.3%; (b) 6%TGIC-DOPO/DGEBA/DDS, residual weight:15.7%; (c) 8%TGIC-DOPO/DGEBA/DDS, residual weight:16.1%; (d) 10%TGIC-DOPO/DGEBA/DDS, residual weight:17.5%; (e) 12%TGIC-DOPO/DGEBA/DDS, residual weight:17.8%.

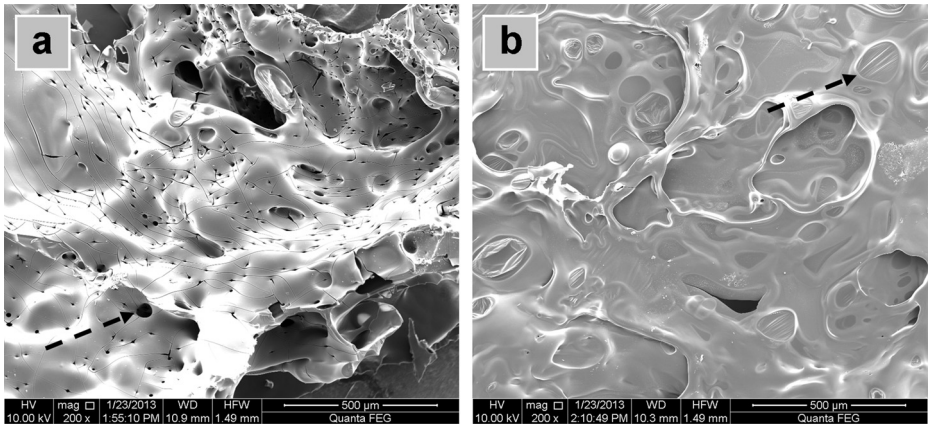

Fig. 4. SEM photos of the cone calorimeter residues. (a) DGEBA/DDS and (b) 12%TGIC-DOPO/DGEBA/DDS.

phase contributes to the better flame-retardant properties of matrix.

3.5. Pyrolysis behavior of TGIC-DOPO

To further explore the pyrolysis behavior and its flame-retardant mechanism of TGIC-DOPO, the Py-GC-MS was adopted with a pyrolysis temperature at 500 °C. The MS spectra of TGIC-DOPO are shown in Fig. 5. In accordance with the chemical structure of TGIC-DOPO shown in Scheme 1 and the typical m/z values provided in Fig. 5, the deduced pyrolysis route of TGIC-DOPO is illustrated in Fig. 6. TGIC-DOPO molecules were firstly decomposed into two main parts: tri-allyl-triazine-trione piece (m/z = 249) and phosphaphenanthrene fragments (m/z = 230 or 215). Then the pyrolysis process would proceed separately. On one hand, the further pyrolysis of two kinds of phosphaphenanthrene fragments would generate several kinds of inert free radicals with quenching effect, such as phenoxyl free radical (m/z = 93), (phenyl, methyl)-phosphoryl free radical (m/z = 139), •PO_2 free radical (m/z = 63), •PO free radical (m/z = 47), biphenyl free radical (m/z = 152) and o-phenyl-phenoxyl free radical (m/z = 169). On the other hand, the further pyrolysis of tri-allyl-triazine-trione fragment would generate a series of inert alkyl isocyanate free radicals (m/z = 208, 125, 83, 70, 56) and also active allyl radical (m/z = 41). The deduced structures of all the mentioned fragments were illustrated in Fig. 6. During the pyrolysis process of TGIC-DOPO, most of the pyrolysis fragments were inert free radicals which can capture and quench the active chain reaction free radicals from the decomposed matrix, such as •OH, •H and hydrocarbon free radicals, and then inhibiting the gaseous-phase combustion process. The inert free radicals of TGIC-DOPO can also combine with the molecular chains of matrix containing active terminal free radical, and then prevent matrix from further degradation. Therefore, TGIC-DOPO exerts the flame-retardant effect both in gaseous phase and condensed phase.

Table 5
XPS data of residues from the cone calorimeter.

Samples	Element content (wt.%)				
	C	N	O	P	S
DGEBA/DDS	80.76	6.30	12.31	0.15	0.49
6%TGIC-DOPO/DGEBA/DDS	76.49	5.47	15.43	1.62	1.00
8%TGIC-DOPO/DGEBA/DDS	77.82	5.51	13.87	1.58	1.23
10%TGIC-DOPO/DGEBA/DDS	77.78	4.36	14.97	1.73	1.35
12%TGIC-DOPO/DGEBA/DDS	76.92	4.04	15.96	1.86	1.22

3.6. Flame-retardant mechanism of TGIC-DOPO in DGEBA thermosets

According to all the discussed results, the flame-retardant mechanism of TGIC-DOPO in DGEBA thermosets is concluded as follows. TGIC-DOPO decomposed at the lower temperature and induced the matrix to decompose in advance, which contributed to the formation of the phosphorus-rich residues. The phosphorus-rich residues increase the toughness of residue melt and inhibit heat and flammable gas from exchanging. The pyrolysis of TGIC-DOPO also released various fragments with quenching effect. The fragments effectively enhanced the flame-retardant performance in gaseous phase during combustion, such as the higher LOI value of thermosets, the lower HRR and EHC values. The inert fragments with quenching effect also promoted quenching more molecular chains with active terminal free radical from matrix and more compositions would be reserved in residue, which was consistent with the higher flame-retardant rating and residual char yields. Therefore, the quenching effect of TGIC-DOPO can exert the flame-retardant effect both in gas phase and condensed phase. But the flame retardant effect of TGIC-DOPO will be redistributed under the different conditions. With increasing mass fraction of TGIC-DOPO in DGEBA thermosets, the more phosphaphenanthrene groups were reserved in residues to exert the condensed-phase flame-retardant effect, and the more triazine-trione groups were

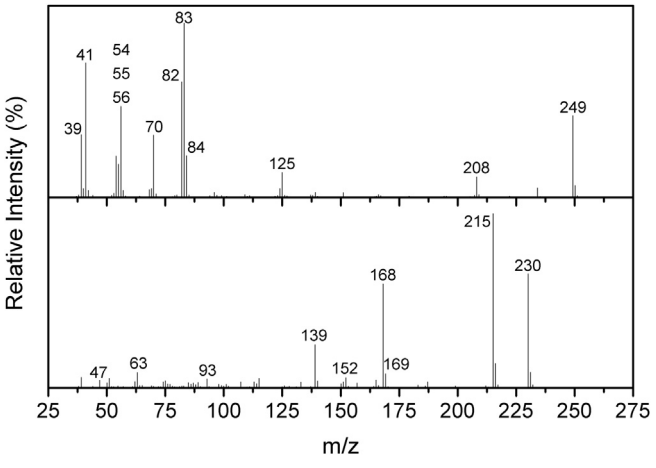

Fig. 5. MS spectra of main fragments of the pyrolyzed TGIC-DOPO at 500 °C.

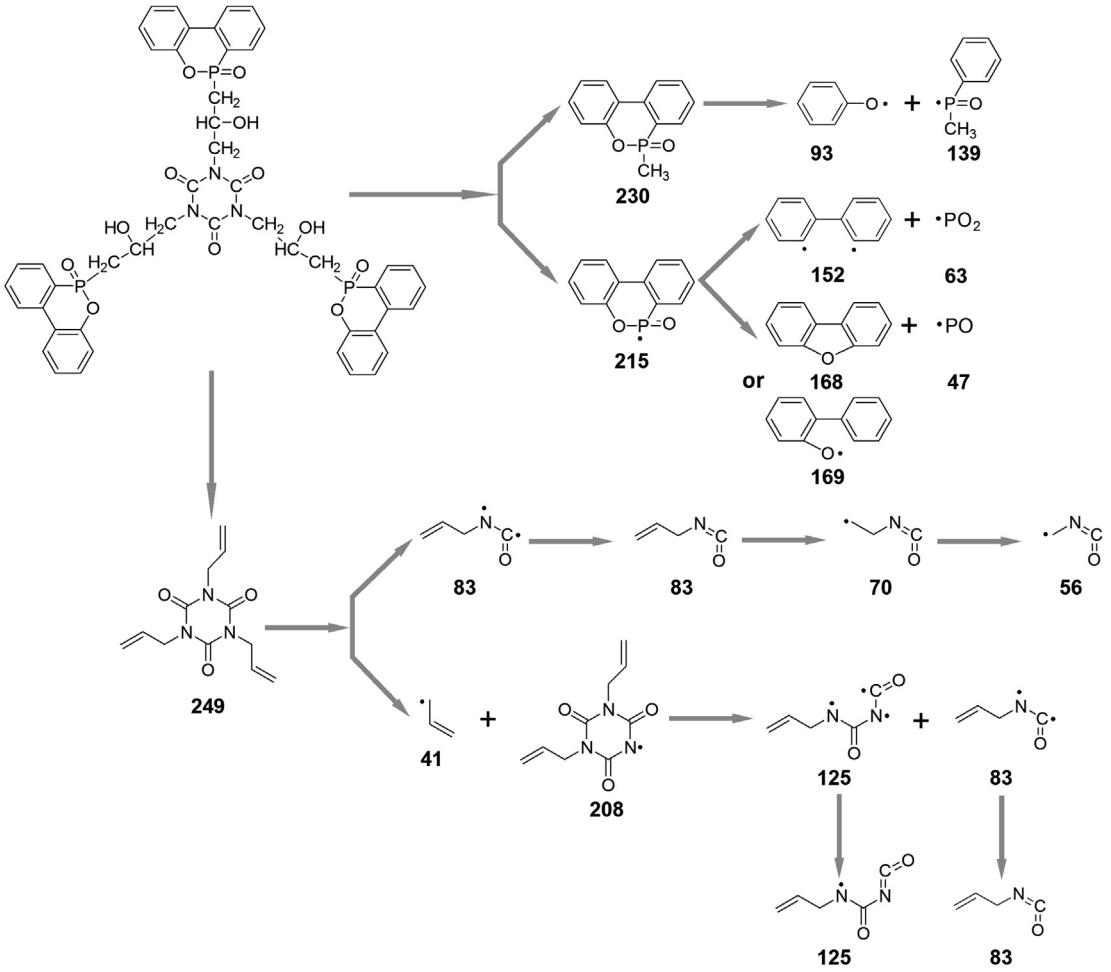

Fig. 6. The deduced pyrolysis route of TGIC-DOPO.

decomposed into inert fragments to play the role of gaseous-phase flame-retardant effect. Therefore, the flame-retardant performance of TGIC-DOPO is resulted by the synergistic effect of phosphaphenanthrene and triazine-trione groups.

4. Conclusion

A novel flame retardant additive, TGIC-DOPO, which was constructed by phosphaphenanthrene and triazine-trione groups, was synthesized and characterized. TGIC-DOPO showed outstanding flame-retardant effect on the DGEBA thermoset because of the existence of phosphaphenanthrene and triazine-trione groups. This observation was confirmed by the results of the LOI flammability, vertical burning, and cone calorimeter tests. Specifically, the thermoset had an LOI value of 33.3% when the mass fraction of TGIC-DOPO was only 6wt.%. When the mass fraction of TGIC-DOPO reached 12wt.%, 12%TGIC-DOPO/DGEBA/DDS specimen reached the UL94 V-0 rating. The pyrolysis of TGIC-DOPO can release various fragments with quenching effect, which effectively enhanced the LOI values of thermosets and reduced the HRR and EHC values and which also contributed to the higher flame-retardant rating, the higher residual char yields and the stronger toughness of melt. TGIC-DOPO possesses the flame-retardant effect both in gaseous phase and condensed phase during combustion. With increasing mass fraction of TGIC-DOPO in DGEBA thermosets, the more phosphaphenanthrene groups exerted the condensed-phase flame-retardant effect, and the more triazine-trione groups played the role of gaseous-phase flame-retardant effect. The redistribution of flame-retardant effect confirms the synergistic effect of phosphaphenanthrene and triazine-trione groups.

Acknowledgments

Financial support was provided by the National Nature Science Foundations (No. 21374003 and No. 51103002) and the Education Science & Research Development Project of Beijing Municipal Institutions (No. KM201110011010).

References

[1] Raquez JM, Deléglise M, Lacrampe MF, Krawczak P. Thermosetting (bio)materials derived from renewable resources: a critical review. Prog Polym Sci 2010;35(4):487–509.
[2] Dasari A, Yu ZZ, Cai GP, Mai YW. Recent developments in the fire retardancy of polymeric materials. Prog Polym Sci 2013;38(9):1357–87.
[3] Santhosh Kumar KS, Biju R, Reghunadhan Nai CP. Progress in shape memory epoxy resins. React Funct Polym 2013;73(2):421–30.
[4] Mohan P. A critical review: the modification, properties, and applications of epoxy resins. Polym-Plast Technol 2013;52(2):107–25.
[5] Odegard GM, Bandyopadhyay A. Physical aging of epoxy polymers and their composites. J Polym Sci Pol Phys 2011;49(24):1695–716.
[6] Rosca ID, Hoa SV. Method for reducing contact resistivity of carbon nanotube-containing epoxy adhesives for aerospace applications. Compos Sci Technol 2011;71(2):95–100.
[7] Massoumi B, Farjadbeh F, Mohammadi R, Entezami AA. Synthesis of conductive adhesives based on epoxy resin/nanopolyaniline and chloroprene rubber/

nanopolyaniline: characterization of thermal, mechanical and electrical properties. J Compos Mater 2013;47(9):1185–95.
[8] Ho TH, Wang CS. Modification of epoxy resin with siloxane containing phenol aralkyl epoxy resin for electronic encapsulation application. Eur Polym J 2001;37(2):267–74.
[9] Gao N, Liu WQ, Ma SQ, Tang CY, Yan ZL. Cycloaliphatic epoxy resin modified by two kinds of oligo-fluorosiloxanes for potential application in light-emitting diode (LED) encapsulation. J Polym Res 2012;19(8):9923.
[10] Bourbigot S, Duquesne S. Fire retardant polymers: recent developments and opportunities. J Mater Chem 2007;17:2283–300.
[11] Rakotomalala M, Wagner S, Döring M. Recent developments in halogen free flame retardants for epoxy resins for electrical and electronic applications. Materials 2010;3(8):4300–27.
[12] Levchik SV, Weil ED. A review of recent progress in phosphorus-based flame retardants. J Fire Sci 2006;24(5):345–64.
[13] Wang CS, Lee MC. Synthesis and properties of epoxy resins containing 2-(6-oxid-6H-dibenz(c,e)(1,2) oxaphosphorin-6-yl) 1,4-benzenediol (II). Polymer 2000;41(10):3631–8.
[14] Jirasutsakul I, Paosawatyanyong B, Bhanthumnavin W. Aromatic phosphorodiamidate curing agent for epoxy resin coating with flame-retarding properties. Prog Org Coat 2013;76(12):1738–46.
[15] Chang HC, Lin HT, Lin CH, Su WC. Facile preparation of a phosphinated bisphenol and its low water-absorption epoxy resins for halogen-free copper clad laminates. Polym Degrad Stab 2013;98(1):102–8.
[16] Wang CS, Lin CH. Synthesis and properties of phosphorus-containing epoxy resins by novel method. J Polym Sci Polym Chem 1999;37(21):3903–9.
[17] Meenakshi KS, Pradeep Jaya Sudhan E, Ananda Kumar S, Umapathy MJ. Development and characterization of novel DOPO based phosphorus tetraglycidyl epoxy nanocomposites for aerospace applications. Prog Org Coat 2011;72(3):402–9.
[18] Perret B, Schartel B, Stöß K, Ciesielski M, Diederichs J, Döring M, et al. Novel DOPO-based flame retardants in high-performance carbon fibre epoxy composites for aviation. Eur Polym J 2011;47(5):1081–9.
[19] El Gouri M, El Bachiri A, Hegazi SE, Rafik M, El Harfi A. Thermal degradation of a reactive flame retardant based on cyclotriphosphazene and its blend with DGEBA epoxy resin. Polym Degrad Stab 2009;94(11):2101–6.
[20] Qian LJ, Ye LJ, Xu GZ, Liu J, Guo JQ. The non-halogen flame retardant epoxy resin based on a novel compound with phosphaphenanthrene and cyclotriphosphazene double functional groups. Polym Degrad Stab 2011;96(6):1118–24.
[21] Zhang WC, Li XM, Yang RJ. Pyrolysis and fire behaviour of epoxy resin composites based on a phosphorus-containing polyhedral oligomeric silsesquioxane (DOPO-POSS). Polym Degrad Stab 2011;96(10):1821–32.
[22] Gao M, Yang SS. A novel intumescent flame-retardant epoxy resins system. J Appl Polym Sci 2010;115(4):2346–51.
[23] Wang X, Hu Y, Song L, Yang HY, Xing WY, Lu HD. Synthesis and characterization of a DOPO-substitued organophosphorus oligomer and its application in flame retardant epoxy resins. Prog Org Coat 2011;71(1):72–82.
[24] Wang X, Hu Y, Song L, Xing WY, Lu HD, Lv P, et al. Effect of a triazine ring-containing charring agent on fire retardancy and thermal degradation of intumescent flame retardant epoxy resins. Polym Adv Technol 2011;22(12):2480–7.
[25] Xiong YQ, Jiang ZJ, Xie YY, Zhang XY, Xu WJ. Development of a DOPO-containing melamine epoxy hardeners and its thermal and flame-retardant properties of cured products. J Appl Polym Sci 2013;127(6):4352–8.
[26] Perret B, Schartel B, Stöß K, Ciesielski M, Diederichs J, Döring M, et al. A new halogen-free flame retardant based on 9,10-dihydro-9-oxa-10-phosphaphenanthrene-10-oxide for epoxy resins and their carbon fiber composites for the automotive and aviation industries. Macromol Mater Eng 2011;296(1):14–30.
[27] Schartel B, Balabanovich AI, Braun U, Knoll U, Artner J, Ciesielski M, et al. Pyrolysis of epoxy resins and fire behavior of epoxy resin composites flame-retarded with 9,10-dihydro-9-oxa-10-phosphaphenanthrene-10-oxide additives. J Appl Polym Sci 2007;104(4):2260–9.
[28] Zang L, Wagner S, Ciesielski M, Müller P, Döring M. Novel star-shaped and hyperbranched phosphorus-containing flame retardants in epoxy resins. Polym Adv Technol 2011;22(7):1182–91.
[29] Qian LJ, Ye LJ, Qiu Y, Qu SR. Thermal degradation behavior of the compound containing phosphaphenanthrene and phosphazene groups and its flame retardant mechanism on epoxy resin. Polymer 2011;52(24):5486–93.